



LAWRENCE
LIVERMORE
NATIONAL
LABORATORY

Moisture Corrosion of LiH: A Kinetic Investigation by DRIFT Spectroscopy

S. M. Matt, J. M. Haschke, W. McLean, L. N. Dinh

June 19, 2019

The Journal of Chemical Physics

Disclaimer

This document was prepared as an account of work sponsored by an agency of the United States government. Neither the United States government nor Lawrence Livermore National Security, LLC, nor any of their employees makes any warranty, expressed or implied, or assumes any legal liability or responsibility for the accuracy, completeness, or usefulness of any information, apparatus, product, or process disclosed, or represents that its use would not infringe privately owned rights. Reference herein to any specific commercial product, process, or service by trade name, trademark, manufacturer, or otherwise does not necessarily constitute or imply its endorsement, recommendation, or favoring by the United States government or Lawrence Livermore National Security, LLC. The views and opinions of authors expressed herein do not necessarily state or reflect those of the United States government or Lawrence Livermore National Security, LLC, and shall not be used for advertising or product endorsement purposes.

Moisture Corrosion of LiH: A Kinetic Investigation by DRIFT Spectroscopy

*Sarah M. Matt, John M. Haschke, William McLean, II, Long N. Dinh**

Lawrence Livermore National Laboratory, 7000 East Ave, Livermore, CA 94550-9234

ABSTRACT

Lithium hydride (LiH) is a unique, ionic compound with applications in a variety of industries. Unfortunately, LiH is very reactive toward H₂O even at ppm levels, forming oxide (Li₂O) and hydroxide (LiOH) corrosion layers while outgassing H₂. An effective means to eliminate unwanted outgassing is vacuum-heating to convert LiOH into Li₂O, although subsequent re-exposure to moisture during transport/handling reconverts some Li₂O back to LiOH. A corrosion growth model for previously vacuum-baked LiH is necessary for long term prediction of the hydrolysis of LiH. In this work, a para-linear hydroxide corrosion growth model is proposed for the reaction of previously vacuum-baked LiH samples with moisture. This model, composed of two competing diffusion reaction fronts at the LiOH/Li₂O and Li₂O/LiH interfaces, is validated experimentally by subjecting a previously vacuum-baked polycrystalline LiH sample to 35 ppm of H₂O at room temperature while monitoring the corrosion growth as a function of time with diffuse-reflectance

infrared Fourier transform (DRIFT) spectroscopy. The para-linear growth model for the hydrolysis of previously vacuum-baked LiH proposed in this report can also serve as a template for the hydrolysis of other hygroscopic oxides grown on metal or metal hydride substrates.

INTRODUCTION

Due to the combination of high hydrogen content and low material density, LiH has prompted significant research and applications across a variety of fields, including hydrogen storage, lightweight neutron shielding in nuclear reactors, and chemical synthesis.¹⁻⁸ But, the applicability as a hydrogen storage material is limited by hydrogen release processes which require heating above 900°C, or through the irreversible corrosive reaction with water.^{1, 5-6} Nonetheless, LiH is used in the synthesis of other, more-promising hydrogen storage materials, and more generally as a reducing agent in chemical synthesis.^{3, 7}

Unfortunately, LiH has a high affinity for water, which is often a detriment for applications and complicates handling and use. There has been significant research on the reactions of LiH with moisture and the subsequent corrosion products. A consensus in the literature is that, at low moisture content, the primary products form a tri-layer system of LiOH / Li₂O / LiH.⁹⁻¹⁰ In a closed vacuum/dry system, a portion of the hydroxide corrosion layer thermally decomposes to form Li₂O while releasing H₂O, which then reacts with LiH, causing unplanned H₂ outgassing.^{4, 7} So, there is a need to quantify the unwanted corrosion layer on LiH due to moisture exposure. One common tool to track this corrosion reaction is diffuse-reflectance infrared Fourier transform (DRIFT) spectroscopic observation of the O-H stretching vibrational mode of LiOH, and this technique is also used in this work.¹¹⁻¹³

Varying proposals about whether the corrosion reaction rate is controlled by diffusion, microcracking, lattice diffusion, and/or other concepts were reviewed and provide a useful overview of the complexity of this issue.^{7, 9-10, 13} The chemical reactions, kinetics and parameters describing the moisture corrosion of pristine LiH were previously reviewed.⁹ However, there is no corrosion growth model for previously vacuum-baked LiH, which practically exposes Li₂O covered LiH samples to moisture.

In this report, the corrosion growth of previously vacuum-baked LiH upon moisture exposure was monitored with DRIFT spectroscopy and a para-linear corrosion growth model was proposed and validated against experimental DRIFT data. The growth kinetics were then extracted based on the rate limiting mechanisms to provide long term prediction. The proposed para-linear growth model in this report can also be used to model the hydrolysis of hygroscopic oxides grown on metal or metal hydride substrates.

EXPERIMENTAL METHODS

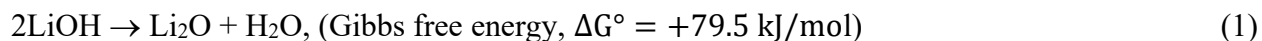
In DRIFT spectroscopy, only the diffuse reflectance, which contains information on the infrared absorption characteristics of the molecular vibration modes present in the sample under investigation, is sent to the detector. As such, DRIFT is an infrared absorption technique for opaque samples.¹⁴ In this work, DRIFT spectra were obtained with a Harrick Scientific Praying Mantis DRIFT chamber fitted inside a Nicolet 4700 series Fourier transform infrared (FTIR) benchtop system. This DRIFT system was capable of 1.33×10^{-4} Pa vacuum and in-situ heating.

Initially, a polycrystalline LiH sample was vacuum-baked (1.33×10^{-4} Pa, 423K to 573K) to convert any existing hydroxide corrosion into Li₂O, as verified by DRIFT upon cooling down to room temperature (~295K). The sample was then exposed to 3.5 Pa of H₂O (equivalent to 35

ppm moisture) inside the DRIFT chamber via a pressure controller connected to a heated pure H₂O source over the course of nearly two months. 32 spectra were periodically acquired from the sample surface with a spectral resolution of ~4 cm⁻¹. All spectra were baseline corrected in the 3400 – 3800 cm⁻¹ spectral region for the analyses in this report.

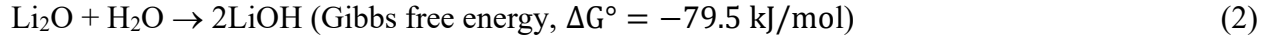
THEORETICAL METHODS

As illustrated in Fig. 1, there are three main stages being considered in the corrosion growth of a previously vacuum-baked LiH sample: 1. Vacuum-baking conversion of LiOH into Li₂O, 2. Gradual reformation of LiOH back from Li₂O, and 3. Further growth of LiOH due to prolonged moisture exposure. The goal of the high temperature vacuum-baking in stage 1 was to eliminate existing moisture potential (in the form of hydroxide). The hydroxide to oxide conversion can be written as:



The large positive Gibbs free energy¹⁵ for reaction (1) means that the reaction is thermodynamically unfavorable, thus vacuum and heat are required to transform the LiOH to Li₂O. It should also be noted that the Li₂O layer in Fig. 1 includes a few cracks. The LiOH tetragonal structure has lattice parameters of a = 0.3553 nm and c = 0.4348 nm while Li₂O has a cubic structure with a = 0.4611 nm. Crack formation to relieve stress is possible during the vacuum-heating and subsequent cooling if the initial hydroxide is thick and/or the heating/cooling rates are aggressive. In Fig. 1, some crack lines are deliberately drawn into the corrosion layer after the vacuum-baking step to represent this possibility. These cracks provide additional H₂O transport paths for the re-conversion of the Li₂O layer back into LiOH during subsequent moisture re-exposure in stage 2.

The gradual reformation of LiOH in stage 2 simulates unavoidable moisture re-exposure during subsequent transport/handling of LiH after the vacuum-heating step. The rehydration can be written as:

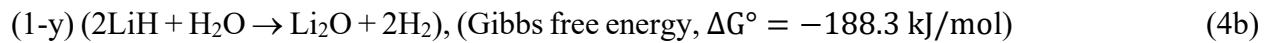


The large negative Gibbs free energy for reaction (2) means that the reaction is thermodynamically favorable. However, once a thin layer of LiOH is formed, further conversion of Li₂O to LiOH happens at the LiOH/Li₂O interface, as opposed to the surface. As such, the rate limiting step becomes the diffusion of H₂O (or OH⁻) through the growing LiOH layer. A square root of time dependence for the LiOH growth is expected for this stage based on the classical diffusion equation:

$$x = \sqrt{2Dt} \quad (3)$$

In equation (3), x is the LiOH thickness, D is the diffusion coefficient of the diffusing species (most probably, OH⁻) through the LiOH layer, and t is time.

As reaction (2) consumes Li₂O at the LiOH/Li₂O interface, the Li₂O buffer layer between LiOH and LiH becomes thin enough to support another competing reaction which forms Li₂O at the LiH/Li₂O interface. The two competing reactions are written in equations 4 (a) and (b) below:

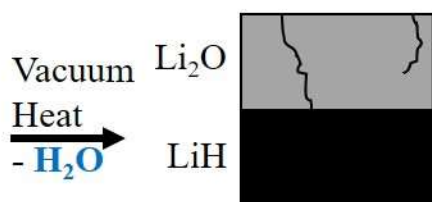
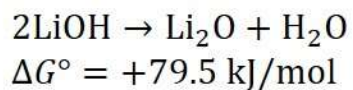


In equations 4 (a) and (b), y denotes the equivalent mole fraction of H₂O (more likely in the form of OH⁻ + H⁺) that reaches the LiOH/Li₂O interface. At the beginning of moisture re-exposure in stage 2, y = 1 and the reaction to destroy Li₂O to reform LiOH in equation 4(a) is exclusive. With continued H₂O exposure time, as the Li₂O layer becomes thinner and the LiOH layer gets thicker, the value of y decreases, allowing (1-y) equivalent mole fraction of H₂O to reach the Li₂O/LiH

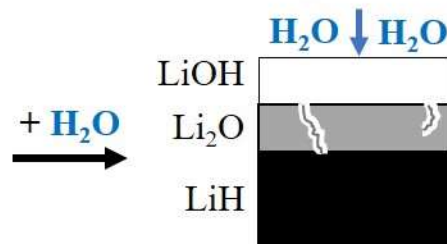
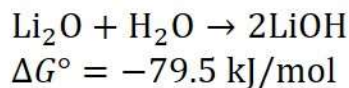
interface and form Li_2O plus H_2 as described in equation 4(b). With even more H_2O re-exposure, a point is reached such that $y = 0.5$ and $(1-y) = 0.5$ causing equal formation and destruction of Li_2O at opposite interfaces. This results in further growth of the LiOH corrosion layer while the thin Li_2O layer remains constant (stage 3) thereafter until the LiH substrate is completely consumed.

During stage 3 of the corrosion growth, the rate limiting step is diffusion of OH^- or O^{2-} through the constant-thickness Li_2O layer and proceeds with simultaneous outward diffusion of H^- . Hydrogen is removed from LiH and charge balance is maintained in the Li_2O layer during the reaction. In one possible mechanism, H_2O is transported to the $\text{Li}_2\text{O}/\text{LiH}$ interface as $\text{H}^+ + \text{OH}^-$ and 2H_2 is formed and transported to the $\text{LiOH}/\text{Li}_2\text{O}$ interface as $\text{H}^+ + \text{H}^-$. In the other mechanism, O^{2-} is formed at the $\text{LiOH}/\text{Li}_2\text{O}$ interface by reaction of 2OH^- to form 2H^+ and O^{2-} . As O^{2-} diffuses to the $\text{Li}_2\text{O}/\text{LiH}$ interface, charge balance is maintained by diffusion of 2H^- from LiH to the $\text{LiOH}/\text{Li}_2\text{O}$ interface. In either case, a steady-state (constant-thickness) Li_2O layer is maintained by opposing reactions (formation and consumption of Li_2O) that occur at equal rates via a kinetically controlled mechanism. Although the exact nature of the diffusing/reactant species is beyond the scope of this work, the rate limiting step is the diffusion of a reactant species through the thin Li_2O layer of constant thickness.⁷ Thus, the LiOH growth rate is linear and proportional to $2D^*/\text{Li}_2\text{O}$ thickness (where D^* is the diffusion coefficient of the reactant diffusing through the Li_2O layer).

1. Vacuum Bakeout



2. Conversion of Oxide to Hydroxide



3. Hydroxide Growth from LiH

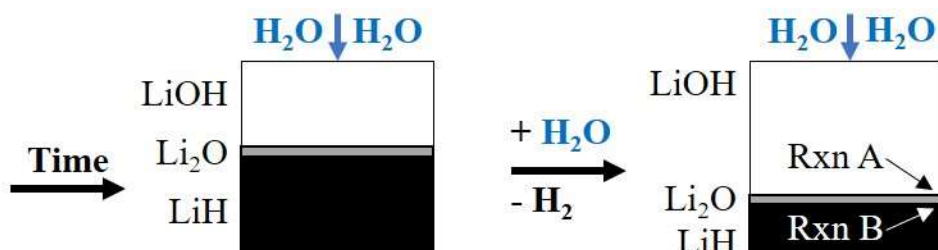
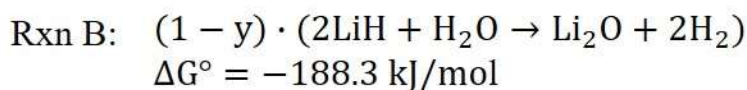
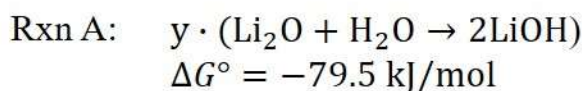


Figure 1. The corrosion growth of a previously vacuum-baked LiH sample: 1. Vacuum-baking conversion of LiOH into Li_2O , 2. Diffusion-limited gradual reformation of LiOH back from Li_2O , and 3. Further growth of LiOH with a constant Li_2O thickness due to prolonged moisture exposure.

RESULTS AND DISCUSSION

The main O-H stretching vibrational mode of LiOH appears in the background-subtracted DRIFT spectra presented in Fig. 2 at $\sim 3676 \text{ cm}^{-1}$ and increases in intensity with continued moisture exposure. The 3676 cm^{-1} peak is always observed for LiOH grown on both as-received LiH and

vacuum-baked LiH. An expanded view of the growth of the main LiOH peak at 3676 cm^{-1} with respect to exposure time is shown in the inset of Fig. 2. This main LiOH peak contains two spectral features: a larger, higher frequency peak and a small shoulder on the lower frequency side. The largest peak is denoted as bulk state ($3676 \pm 1\text{ cm}^{-1}$), the smaller shoulder on the lower frequency side is denoted as surface state ($3666 \pm 7\text{ cm}^{-1}$). These two distinct spectral features are most clearly visible at very early times. In addition, at much lower wavenumber ($3526 \pm 1\text{ cm}^{-1}$), a smaller peak is observed only on some previously vacuum-baked samples after re-exposure to moisture which is denoted as interfacial LiOH state. Due to the shift to lower wavenumbers from bulk LiOH state to surface LiOH state and then to interfacial LiOH state, the thermal stability is expected to reduce in that order in agreement with ref. 10. Bulk LiOH state is associated with crystalline LiOH and is thermally very stable, while it requires less energy to break bonds among LiOH molecules in defective or non-crystalline portions (so-called surface LiOH state) of the LiOH layer grown on LiH at room temperature.¹⁰ The interfacial LiOH state is least thermally stable simply because of its close proximity to the reducing LiH substrate, which weakens the OH bonds.¹⁰ The densities and crystal structures of LiH, Li₂O, and LiOH are given in Table 1.

Table 1: Densities and crystal structures of LiH, Li₂O, and LiOH.

	LiH	Li₂O	LiOH
Density (g/cm³)	0.82	2.01	1.46
Crystal Structure	Face-Centered Cubic	Cubic	Tetragonal
Lattice Parameter	a = 0.40834 nm	a = 0.4611 nm	a = 0.3553 nm c = 0.4348 nm

During the vacuum-baking process described by reaction (1), some H₂O, generated by heating LiOH, moves toward LiH and reacts with it to form more Li₂O according to reaction 4(b).¹⁰ The volume expansion in transforming LiH to Li₂O during the vacuum-baking process tends to create cracks to relieve stress when the heating rate is fast and/or the corrosion layer is thick. For the crack lines that extend from the sample surface to near the LiH substrate, they act as tunnels to supply H₂O during subsequent moisture re-exposure to reform LiOH from Li₂O at locations far ahead of the main LiOH/Li₂O reaction front (see top right illustration in Fig. 1). In this way, the LiOH formed near the Li₂O/LiH interface exists essentially as LiOH islands in a Li₂O matrix and, due to its proximity to LiH, is identified as the interfacial LiOH state which manifests in DRIFT spectra as the smaller 3526 cm⁻¹ peak. This shift to lower wavenumber OH vibrational modes indicates that the interfacial LiOH state is less thermally stable than that located within the main LiOH region. Indeed, the OH DRIFT peak at 3526 cm⁻¹ decreases in intensity even at room temperature in a vacuum/dry environment over a period of many months and completely disappears upon vacuum-heating to 343K. Even though the peak wavenumber of interfacial LiOH state is similar to that of LiOH·H₂O (3526 cm⁻¹ vs 3570 cm⁻¹),¹¹ the interfacial LiOH state is much more thermally stable than LiOH·H₂O which has been observed to completely disappear in a vacuum/dry environment at room temperature in only one to two days, instead of many months for interfacial LiOH state.¹⁶

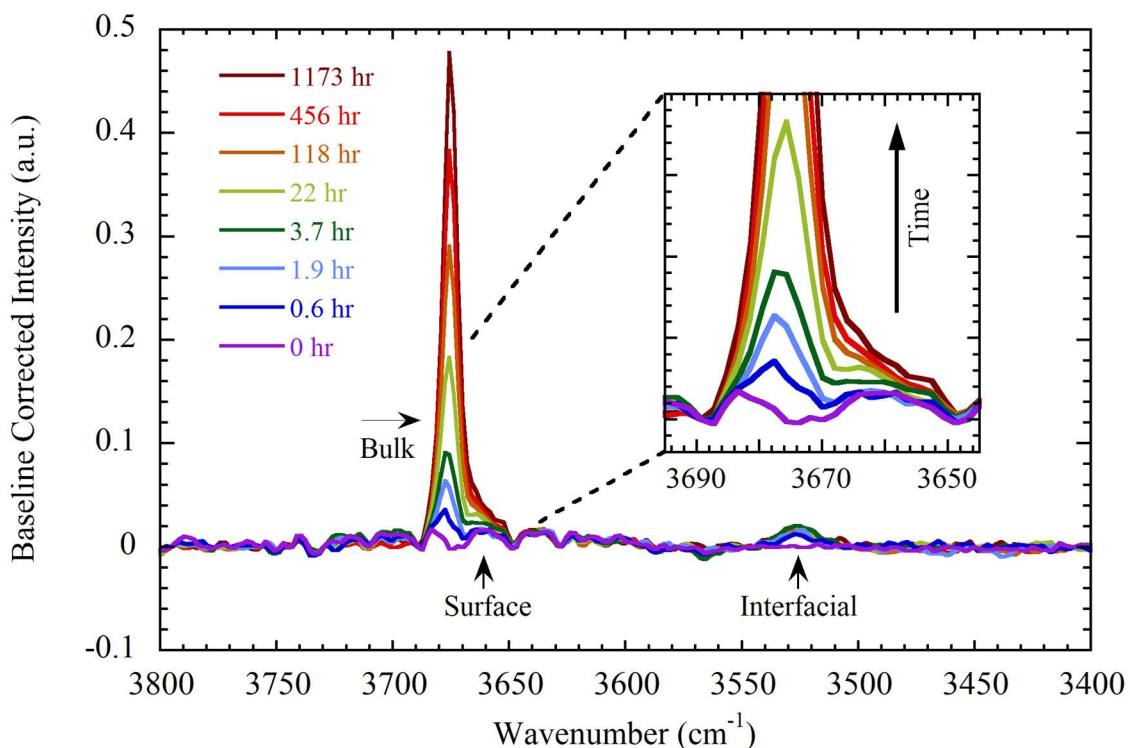


Figure 2. Background-subtracted DRIFT spectra showing LiOH growth on LiH surface at 295K in 35 ppm H₂O. The main OH stretching vibrational mode (bulk LiOH state) appears around 3676 cm⁻¹. The smaller shoulder on the lower frequency side is denoted as surface state (3666 ± 7 cm⁻¹). The small peak at 3526 cm⁻¹ originates from LiOH interfacial state (formed near LiH substrate due to cracks extending from sample's geometrical surface to near the Li₂O/LiH interface). The inset shows the expanded view of the evolution of the ~3676 cm⁻¹ peak with time.

The time evolution of the three hydroxyl DRIFT peaks (bulk, surface and interfacial states) are plotted in Fig. 3. After an initially fast increase, the LiOH interfacial state (red) became nearly constant with time. The initially fast increase in DRIFT peak intensity at 3526 cm⁻¹ is consistent with fast H₂O transport along cracks to near the LiH/Li₂O interface. However, the DRIFT intensity

for the interfacial LiOH state at 3526 cm^{-1} quickly reached a steady intensity due to the finite number of cracks near the LiH interface. In contrast, the bulk LiOH state peak at 3676 cm^{-1} increased rapidly and continued to grow with further exposure time. For room temperature grown LiOH, the surface and bulk state intensities were comparable at early time (thinner hydroxide region) but progressed to form a significantly smaller surface state to bulk state ratio at later time (thicker hydroxide region). For practical purposes, the LiOH growth kinetics can be approximated by just the dominant bulk LiOH signal at 3676 cm^{-1} .

Panel b is an expanded view of the first few hours of the experiment showing how quickly the interfacial state intensity reached a maximum while the intensity of the main LiOH peak continued to rise. The lines connecting the data points in panel b are included simply to guide the eye.

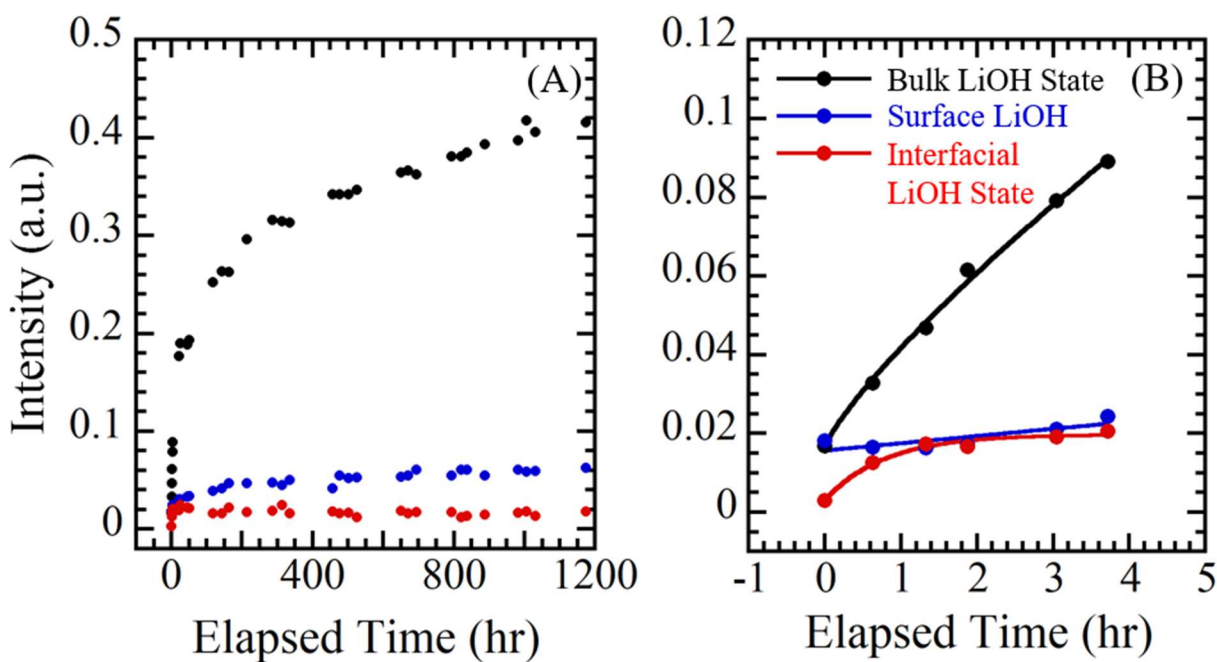


Figure 3. The hydroxide corrosion growth with time as tracked by DRIFT intensities of the bulk LiOH state peak at 3676 cm^{-1} (black dots), the surface LiOH state peak at 3666 cm^{-1} (blue dots), and of the interfacial LiOH state peak at 3526 cm^{-1} (red dots). Panel b is an expanded view of the growth in the first few hours.

With a previous calibration from G.L. Powell (1 a.u. corresponds to 2.4 μm LiOH), a background-subtracted DRIFT spectrum at 3675 cm^{-1} for LiH can be correlated to the thickness of the growing LiOH layer (private communications). Specifically, the time-dependent trend in Fig. 4 is obtained by multiplying the intensity of the acquired and processed spectra by 2.4×10^{-4} cm/au and plotting with respect to total elapsed time in seconds. This choice of units enables comparison of extracted kinetic parameters to previous work. After almost two months of exposure to 35 ppm of H_2O at room temperature, the calculated LiOH corrosion layer was ~ 1.2 μm thick. The overall rate of moisture corrosion of LiH under the low moisture condition of this work can be described as para-linear. The data in the first $\sim 1.8 \times 10^5$ seconds (~ 50 hours) fit very well with a one dimensional (1D) diffusion equation of the form $x = \sqrt{2Dt}$ where x is the LiOH thickness in cm, D is the diffusion coefficient in cm^2/s , and t is time in seconds. Stage 2 of the proposed mechanism in Fig. 1 advances by diffusion of H_2O (more likely as OH^-) through the growing LiOH layer. The best-fit parameters extracted from this data result in $D = 9.85 \times 10^{-15}$ cm^2/s under the condition of 35 ppm H_2O at room temperature (295K). So, DRIFT data are consistent with the proposed model of reconversion of Li_2O into LiOH (stage 2 in Fig. 1) by diffusion of reactive species (most likely OH^-) through the growing LiOH layer. It is noted here that, despite a common value of the diffusion coefficient, the time it takes to end this parabolic growth region should vary with the thickness of the original corrosion layer. Beginning at $\sim 4.2 \times 10^5$ seconds (~ 117 hours), the remaining data points can be best fitted with a linear function of the form $x = Rt + b$ where $R = 1.14 \times 10^{-11}$ cm/s is the linear growth rate and b is a fitting constant. Such a successful linear fit of the latter portion of DRIFT data is also consistent with the proposed model, which explains the linear growth rate in the later phase of corrosion growth (stage 3 in Fig. 1) as the result of diffusion

of reactive species through a Li₂O layer of constant thickness. This linear growth rate region should continue until all LiH is consumed.

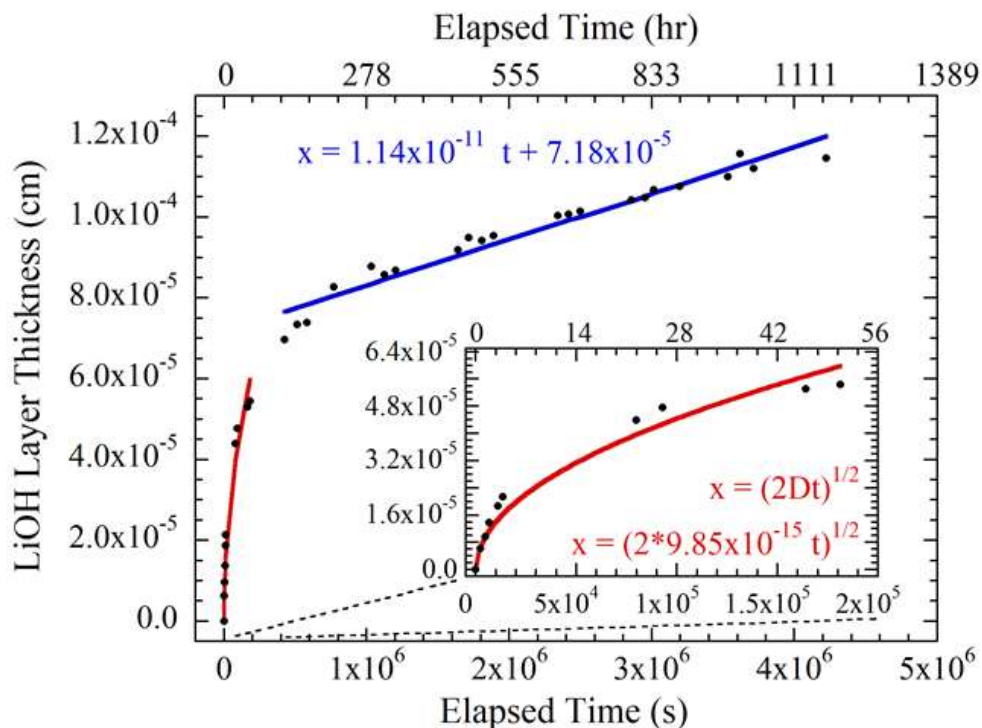


Figure 4. LiOH Layer Growth Rate. The best fit to the initial region up to $\sim 1.8 \times 10^5$ seconds was a one dimensional diffusion model ($x = \sqrt{2Dt}$ where x is the LiOH thickness in cm, D is the diffusion coefficient in cm^2/s , and t is time in seconds). This fitting results in a diffusion coefficient for LiOH of $9.85 \times 10^{-15} \text{ cm}^2/\text{s}$. The latter portion of the experimental data can be best fitted with a linear model with a slope/rate of $1.14 \times 10^{-11} \text{ cm/s}$.

A para-linear corrosion growth model has been previously reported for a clean LiH surface.⁷ In ref. (7), the reaction of a clean LiH surface with very low moisture level produced Li₂O with a thickness defined by the diffusion rates of reactive species through the growing Li₂O layer. According to that study, once the Li₂O layer is thick enough, further reaction with H₂O forms LiOH while maintaining a constant Li₂O thickness through a 2-step reaction. Despite differences

in initial surfaces and the proposed mechanisms (2-step reactions for the prior study and competing reactions for this work) for the maintenance of a constant Li_2O thickness during the linear growth phase, the conclusions of the two studies are complementary. More explicitly, using the reaction factor defined in Fig. 1, the clean LiH surface in the earlier work begins with $y = 0$ for reaction (4b) then increases until $y = 0.5$ as the Li_2O layer grows thicker. In contrast, the system described in this work begins with a thick Li_2O layer such that $y = 1$ and decreases until $y = 0.5$ as the Li_2O layer becomes thinner. For both models, once $y = 0.5$, the rate of Li_2O consumption at the $\text{LiOH}/\text{Li}_2\text{O}$ interface equals the rate of Li_2O formation at the $\text{LiH}/\text{Li}_2\text{O}$ interface, resulting in a linear growth of LiOH and maintenance of a constant Li_2O thickness until complete consumption of LiH .

CONCLUSIONS

The corrosion growth rate of LiOH on initially vacuum-baked LiH after exposure to 35 ppm of H_2O at 295K was monitored using DRIFT spectroscopy. The LiOH corrosion layer was observed to grow in accordance with a para-linear kinetic model. The proposed mechanism accounts for the growth of an LiOH layer after exposure of Li_2O covered LiH to moisture. Transport of reactive species through the LiOH layer is limited by diffusion. This is followed by a linear growth rate as reactive species are transported through a constant-thickness Li_2O layer until consumption of LiH is complete. The proposed mechanism is supported by DRIFT data and provides kinetic parameters for predicting rates. The hydrolysis of other hygroscopic oxides grown on metal or metal hydride substrates may also follow this para-linear kinetic growth model. However, the nature of the diffusing species involved in transport mechanisms of the reaction stages is uncertain and beyond the scope of this study.

AUTHOR INFORMATION

Corresponding Author

*Corresponding author. Tel.: +1 925 422 4271. E-mail address: dinh1@llnl.gov (L.N. Dinh).

ACKNOWLEDGMENT

We acknowledge Elizabeth A. Sangalang for helpful discussions during the preparation of this work. This work was performed under the auspices of the U.S. Department of Energy by Lawrence Livermore National Laboratory under Contract DE-AC52-07NA27344.

REFERENCES

1. Møller, K. T.; Jensen, T. R.; Akiba, E.; Li, H.-W. Hydrogen - A Sustainable Energy Carrier. *Prog. Nat. Sci: Mater. Int.* **2017**, *27*, 34-40.
2. Welch, F. H. Lithium Hydride: A Space Age Shielding Material. *Nucl. Eng. Des.* **1974**, *26*, 444-460.
3. Shitanda, I.; Sato, A.; Itagaki, M.; Watanabe, K.; Koura, N. Electroless Plating of Aluminum Using Diisobutyl Aluminum Hydride as Liquid Reducing Agent in Room-Temperature Ionic Liquid. *Electrochim. Acta* **2009**, *54*, 5889-5893.
4. Tonks, J. P.; King, M. O.; Galloway, E. C.; Watts, J. F. Corrosion Studies Of Lih Thin Films. *J. Nucl. Mater.* **2017**, *484*, 228-235.
5. Vajo, J. J.; Mertens, F.; Ahn, C. C.; Bowman, R. C.; Fultz, B. Altering Hydrogen Storage Properties by Hydride Destabilization through Alloy Formation: LiH and MgH₂ Destabilized with Si. *J. Phys. Chem. B* **2004**, *108*, 13977-13983.
6. Gislou, P.; Prosini, P. P. Devices for Producing Hydrogen via NaBH₄ And LiH Hydrolysis. *Int. J. Hydrogen Energy* **2011**, *36*, 240-246.
7. Haertling, C. L.; Hanrahan, R. J.; Tesmer, J. R. Hydrolysis Studies of Polycrystalline Lithium Hydride. *J. Phys. Chem. C* **2007**, *111*, 1716-1724.
8. Mughabghab, S.; Schmidt, E.; Ludewig, H. Generation of Neutronic Thermal Data in Support of Space Nuclear Propulsion. *AIP Conf. Proc.* **1993**, *271*, 965-971.
9. Haertling, C.; Hanrahan, R. J.; Smith, R. A. Literature Review of Reactions and Kinetics of Lithium Hydride Hydrolysis. *J. Nucl. Mater.* **2006**, *349*, 195-233.
10. Dinh, L. N.; Grant, D. M.; Schildbach, M. A.; Smith, R. A.; Siekhaus, W. J.; Balazs, B.; Leckey, J. H.; Kirkpatrick, J. R.; McLean, W. Kinetic Measurement and Prediction of the Hydrogen Outgassing from the Polycrystalline LiH/Li₂O/LiOH System. *J. Nucl. Mater.* **2005**, *347*, 31-43.

11. Smyrl, N. R.; Fuller, E. L.; Powell, G. L. Monitoring the Heterogeneous Reaction of LiH and LiOH with H₂O and CO₂ by Diffuse Reflectance Infrared Fourier-Transform Spectroscopy. *Appl. Spectrosc.* **1983**, *37*, 38-44.
12. Awbery, R. P.; Broughton, D. A.; Tsang, S. C. In Situ Observation of Lithium Hydride Hydrolysis by DRIFT Spectroscopy. *J. Nucl. Mater.* **2008**, *373*, 94-102.
13. Dinh, L. N.; Schildbach, M. A.; Smith, R. A.; Grant, D. M.; Balazs, B.; McLean II, W. Hydrogen Outgassing from Lithium Hydride. In *Nuclear Materials Research Developments*, Keister, J. E., Ed. Nova Science Publishers, Inc.: New York, 2007; pp 257-283.
14. Blitz, J. P. Diffuse Reflectance Spectroscopy. In *Modern Techniques in Applied Molecular Spectroscopy*, Mirabella, F. M., Ed. John Wiley & Sons: 1998; Vol. 14, pp 185-219.
15. Roine, A. HSC Chemistry® [Software]. Outotec: Pori, Finland, 2018; Software available at www.outotec.com/HSC.
16. Dinh, L. N.; Cecala, C. M.; Leckey, J. H.; Balooch, M. The Effects of Moisture on LiD Single Crystals Studied by Temperature-Programmed Decomposition. *J. Nucl. Mater.* **2001**, *295*, 193-204.

TOC Graphic

